Online Appendix to Winners and Losers: Creative Destruction and the Stock Market

Leonid Kogan* Dimitris Papanikolaou†
Noah Stoffman‡

March 20, 2017

*MIT Sloan School of Management and NBER, lkogan@mit.edu
†Kellogg School of Management and NBER, d-papanikolaou@kellogg.northwestern.edu
‡Kelley School of Business, nstoffma@indiana.edu

Outline

In Section 1 we include some additional results that complement the results in the main paper. In Section 2 we discuss details of the estimation procedure.

1 Additional Results

This section is organized as follows. In Section 1.1 we analyze the cashflow risk implied by the model. In Section 1.2 we demonstrate by the market to book ratio is a good proxy for the firms' technology risk exposures. In Section 1.3 we verify the results of the existing literature on income inequality, which concludes that most of the inequality is within cohorts (O'Rand and Henretta, 2000).

1.1 Cashflow risk

We begin by analyzing the risk properties of the model's implied cashflow process.

1.1.1 Risk and risk prices across horizons

Our model generates a sizable equity premium due to joint movements in aggregate dividends and the stochastic discount factor. Here, we briefly examine how risk at different horizons contributes to asset prices. To do so, we follow Borovička, Hansen, and Scheinkman (2014) and construct shock exposure

$$\varepsilon_q(T-t, X_t) = \eta(X_t) \frac{E_t(D_T \mathcal{M}_t \log D_T | X_t)}{E_t(D_T | X_t)} \tag{1}$$

and shock-price elasticities,

$$\varepsilon_p(T-t, X_t) = \eta(X_t) \frac{E_t(D_T \mathcal{M}_t \log D_T | X_t)}{E_t(D_T | X_t)} - \eta(X_t) \frac{E_t(\pi_T D_T (\mathcal{M}_t \log D_T + \mathcal{M}_t \log \pi_T) | X_t)}{E_t(\pi_T D_T | X_t)}. \tag{2}$$

Here, $\mathcal{M}_t \log D_T$ is a Malliavin derivative – that is, it measures the contribution of a shock dB_t to the stochastic process D at time $T > t$. Here, $\eta(X)$ indexes the direction and size of the shock. Expression (1) is very similar to a non-linear impulse response function; it examines the effect of a shock today to future values of D_t. Expression (2) represents the sensitivity of the expected log return associated with cashflow equal to D_T to a marginal increase in the exposure of that cashflow to a time-t shock. These marginal risk prices potentially vary across horizons based on how the shock D propagates.

We focus on two cashflow processes, the total payout to holders of the market portfolio,

$$D_t = \phi Y_t - I_t - \eta \lambda \nu_t, \tag{3}$$

and the payout accruing from assets in place at time t,

$$D_s^{ap} = p_{Z,s}\, e^{-\delta(s-t)} K_t. \tag{4}$$

Even though aggregate dividends D can potentially become negative, this does not happen near the mean of the stationary distribution of ω. It only happens at extreme ranges of the state space that were not reached across 1,000 model simulations. We compute shock-exposure ε_q and shock-price ε_p elasticities for the two processes D and D^{ap} at the mean of the stationary distribution of ω using Monte Carlo simulations. We plot the estimated elasticities in Figure A.1.

The first two columns show the impulse response ε_q of the two cashflow processes to a technology shock. A positive disembodied shock (x) increases dividends, both for the overall market and for assets in place. By contrast, improvements in technology that are embodied in new vintages (ξ) lead to a decline in aggregate dividends in the short term – as firms fund new investments – and an increase in the long run. By contrast, the cash flows accruing from installed capital falls due to competition – the equilibrium price p_Z falls as the economy acquires more and better new capital. The last two columns show the shock-price elasticities ε_p. We see that the marginal risk prices are essentially flat across horizons.

We conclude that the model's implications about the term structure of risk premia stem mostly from the dynamics of cash flows. We can thus see that the contribution of the dividend dynamics induced by x to the equity premium rises modestly with the horizon. Panel B implies the opposite pattern; the contribution of the dividend dynamics induced by ξ to the equity premium is concentrated in the short and medium run, and the rise in long-run dividends contributes negatively to the equity premium. Thus, the equity premium in the model is concentrated at shorter maturities. In terms of assets in place, the risk due to x is somewhat higher in the short run, while the exposure to ξ-shocks is negative and increases in magnitude with maturity. These patterns imply that, in the model, the value premium is most pronounced at longer maturities.

1.2 Firm risk exposures and the market-to-book ratio

We next examine the extent to which Q is a useful summary statistic for firm risk and risk premia in our model. Recall that a firm's log market-to-book ratio can be written as

$$\log Q_{ft} - \log Q_t = \log\left[\frac{V_t}{V_t + G_t}\,\left(1 + \widetilde{p}(\omega_t)\,\left(\bar{u}_{ft} - 1\right)\right) + \frac{G_t}{P_t + G_t}\frac{\bar{u}_{ft}}{z_{ft}}\left(1 + \widetilde{g}(\omega_t)\,\left(\frac{\lambda_{ft}}{\lambda} - 1\right)\right)\right], \tag{5}$$

Examining (5), we note that a firm's market to book ratio is increasing in the likelihood of future growth λ_f, decreasing in the firm's relative size z_f, and increasing in the firm's current productivity $\bar{u}_f$. This latter effect prevents Tobin's Q from being an ideal measure of growth opportunities, since

it is contaminated with the profitability of existing assets.

To examine the extent to which Q is correlated with technology risk exposures, we examine how changes in the firm's current state $(\lambda_{ft}, k_{ft}, \bar{u}_{ft})$ jointly affect both firm Q and risk exposures. We plot the results in Figure A.2. In each of the three columns, we vary one of the elements of the firm's current state (λ_{ft}, z_{ft}, or $\bar{u}_{ft}$) and keep the other two constant at their steady-state mean. On the horizontal axis, we plot the change in the firm's Q (relative to the market). On the vertical axis we plot the firm's return exposure to x and ξ (panels A and B, respectively) and the firm's risk premium (panel C). We scale the horizontal axis so that it covers the 0.5% and 99.5% of the steady-state distribution of the each of the firm's state variables. The resulting cross-sectional distribution of Tobin's Q is highly skewed.

Examining Figure A.2, we see that regardless of the source of the cross-sectional dispersion in Q, the relation between Q and risk exposures is positive. The pattern in the first two columns is consistent with the impulse responses in the previous section – small firms with high probability of acquiring future projects have higher technology risk exposures than large firms with low growth potential. The last column shows that increasing the firm's current productivity $\bar{u}_f$ – holding λ_f and k_f constant increases both Q and risk exposures. This pattern might seem puzzling initially, since increasing productivity $\bar{u}_f$ while holding size k_f and investment opportunities λ_f constant will lower λ_f/z_f. However, altering $\bar{u}_f$ also has a cashflow duration effect: due to mean reversion in productivity, profitable firms have lower cashflow duration – their cashflows are expected to mean-revert to a lower level. This lower duration of high $\bar{u}_f$ firms implies that their valuations are less sensitive to the rise in discount rates following a positive technology shock– see the response of the interest rate in the paper. In our calibration, this duration effect overcomes the effect due to λ_f/z_f, implying a somewhat more positive stock price response for high-$\bar{u}_f$ firms. However, the magnitude of this effect is quantitatively minor.

The last row of Figure A.2 shows how the firms' risk premium (unlevered) is related to cross-sectional differences in Q. Recall that the two technology shocks carry risk premia of the opposite sign. The disembodied shock carries a positive risk premium; in the absence of other technology shocks, this would imply that firms' risk premia rise with their market-to-book ratio. However, the fact that the embodied shock carries a negative risk premium – coupled with its higher volatility – implies a lower risk premium for growth firms relative to value firms. Households are willing to accept lower average returns for investing in growth firms because doing so allows them to partially hedge the displacement arising from the embodied shock ξ – the decline in their continuation utility.

1.3 The importance of within cohort inequality

An important distinction between our paper and prior work is our focus in within- as opposed to between cohort inequality (Garleanu, Kogan, and Panageas, 2012). The literature on income inequality largely agrees that the degree of within-cohort inequality is an order of magnitude greater

than between-cohort inequality (O'Rand and Henretta, 2000). Also, Song, Price, Guvenen, Bloom, and von Wachter (2015) document that most of the rise in income inequality over the 1978 to 2012 period is within-cohorts.

Here, we show that similar patterns hold if we measure inequality in terms of income, consumption or wealth. To illustrate this point, we compute inequality measures for consumption (using the CEX) and income or wealth (using the SCF). We first remove observation year effects from consumption, income and wealth. We then report the resulting inequality moments before and after removing cohort fixed effects. We also do so separately for the subsample of households that own stocks (since the limited participation model is now the baseline, following your point 6 below). Here, we define cohort effects as the birth year of the leading member of the household.

We deal with the age-cohort-period identification problem in two ways. The first set of columns reports results without any age effects, so assigns the maximum amount of variation to a cohort effect. However, this may be problematic for wealth inequality, since wealth accumulation mechanically grows with age. Hence, the second column reports results after removing a cubic polynomial in age similar to Garleanu et al. (2012). Even then, the linear age effect is not identified, so we set it to zero in order to maximize the explanatory power of cohort effects.

Table A.1 shows that cohort fixed effects explain a quantitatively minor amount of inequality in either consumption, wealth or income inequality—especially at the top of the distribution and among stock market participants. Standard variance decomposition methods assign substantially less than 1% of the overall variation in log income, or wealth to cohort effects, and at most 3% of the overall dispersion in consumption to cohort fixed effects.

2 Model Estimation

We first describe the estimation procedure. We then discuss the sensitivity of the moments to parameters.

2.1 Estimation Details

First, it is convenient to transform some of the parameters of the model. Specifically, we replace the volatility of the idiosyncratic shock with the variance of its ergodic distribution,

$$v \equiv \frac{\sigma_u^2}{2\,\kappa_u - \sigma_u^2}. \tag{6}$$

Further, in place of the project arrival rate parameters $[\lambda_L, \lambda_H]$, we formulate the model in terms of the mean arrival rate,

$$\lambda \equiv \frac{\mu_L}{\mu_L + \mu_H}\lambda_L + \frac{\mu_H}{\mu_L + \mu_H}\lambda_H \tag{7}$$

and the relative difference,

$$\lambda_D \equiv \frac{\lambda_H - \lambda_L}{\lambda}. \tag{8}$$

We estimate the parameter vector p using the simulated minimum distance method (Ingram and Lee, 1991). Denote by X the vector of target statistics in the data and by $\mathcal{X}(p)$ the corresponding statistics generated by the model given parameters p, computed as

$$\mathcal{X}(p) = \frac{1}{S}\sum_{i=1}^{S} \hat{X}_i(p), \tag{9}$$

where $\hat{X}_i(p)$ is the 21×1 vector of statistics computed in one simulation of the model. We simulate the model at a weekly frequency, and time-aggregate the data to form annual observations. Each simulation has 1,000 firms. For each simulation i we first simulate 100 years of data as 'burn-in' to remove the dependence on initial values. We then use the remaining part of that sample, which is chosen to match the longest sample over which the target statistics are computed. Each of these statistic is computed using the same part of the sample as its empirical counterpart. In each iteration we simulate $S = 100$ samples, and simulate pseudo-random variables using the same seed in each iteration.

Our estimate of the parameter vector is given by

$$\hat{p} = \arg\min_{p \in \mathcal{P}} (X - \mathcal{X}(p))' W (X - \mathcal{X}(p)), \tag{10}$$

where $W = diag(XX')^{-1}$ is our choice of weighting matrix that ensures that the estimation method penalizes proportional deviations of the model statistics from their empirical counterparts.

We compute standard errors for the vector of parameter estimates $\hat{p}$ as

$$V(\hat{p}) = \left(1 + \frac{1}{S}\right)\left(\frac{\partial}{\partial p}\mathcal{X}(p)' W \frac{\partial}{\partial p}\mathcal{X}(p)\right)^{-1} \frac{\partial}{\partial p}\mathcal{X}(p)' W' V_X(\hat{p}) W \frac{\partial}{\partial p}\mathcal{X}(p) \left(\frac{\partial}{\partial p}\mathcal{X}(p)' W \frac{\partial}{\partial p}\mathcal{X}(p)\right)^{-1}, \tag{11}$$

where

$$V_X(\hat{p}) = \frac{1}{S}\sum_{i=1}^{S} (\hat{X}_i(\hat{p}) - \mathcal{X}(\hat{p}))(\hat{X}_i(\hat{p}) - \mathcal{X}(\hat{p}))' \tag{12}$$

is the estimate of the sampling variation of the statistics in X computed across simulations.

The standard errors in (11) are computed using the sampling variation of the target statistics across simulations (12). We use (12), rather than the sample covariance matrix, because the statistics that we target are obtained from different datasets (e.g. cross-sectional versus time-series), and we often do not have access to the underlying data. Since not all of these statistics are moments, computing the covariance matrix of these estimates would be challenging even with access to the underlying data. Under the null of the model, the estimate in (12) would coincide with the empirical

estimate. If the model is misspecified, (12) does not need to be a good estimate of the true covariance matrix of X. Partly for these reasons, we specify the weighting matrix as $W = diag(XX')^{-1}$, rather than scaling by the inverse of the sample covariance matrix of X. In principle we could weigh moments by the inverse of (12). However, doing so forces the model to match moments that are precisely estimated but economically less interesting, such as the dispersion in firm profitability or Tobin's Q.

Solving each iteration of the model is computationally costly, and thus computing the minimum (10) using standard methods is infeasible. We therefore use the Radial Basis Function (RBF) algorithm in Björkman and Holmström (2000). The Björkman and Holmström (2000) algorithm first fits a response surface to data by evaluating the objective function at a few points. Then, it searches for a minimum by balancing between local and global search in an iterative fashion. We use a commercial implementation of the RBF algorithm that is available through the TOMLAB optimization package. The RBF algorithm searches for an approximate minimum over a rectangular set. Table A.3 reports the bounds of this set. We confirm that the estimated parameters lie in the interior of the set.

2.2 Robustness: Comparison across restricted models

Tables A.4 and A.5 in this document present the full set of tables from the robustness exercise in Section 3.6 of the paper. See the main text for a discussion of the results.

3 Identification

Here, we discuss the identification of the model's structural parameters. In Figures A.3 through A.7 we plot the Gentzkow and Shapiro (2014) measure of sensitivity of parameters to moments. We report the measure in elasticity form,

$$\hat{\lambda}_{i,j} = \lambda_{i,j} \frac{X^j(\theta)}{\theta^i}, \tag{13}$$

where $\lambda_{i,j}$ is the element of the sensitivity matrix Λ that corresponds to parameter i and moment j. The matrix Λ is computed as

$$\Lambda = -(G'WG)^{-1}G'W \tag{14}$$

where G is the numerical gradient of the sample moments $g(\theta) = X - \mathcal{X}$ and W is the optimal weighting matrix.

References

Björkman, M. and K. Holmström (2000): "Global Optimization of Costly Nonconvex Functions Using Radial Basis Functions," *Optimization and Engineering*, 1, 373–397.

Borovička, J., L. P. Hansen, and J. A. Scheinkman (2014): "Shock elasticities and impulse responses," *Mathematics and Financial Economics*, 8, 333–354.

Garleanu, N., L. Kogan, and S. Panageas (2012): "Displacement Risk and Asset Returns," *Journal of Financial Economics*, 105, 491–510.

Gentzkow, M. and J. M. Shapiro (2014): "Measuring the Sensitivity of Parameter Estimates to Sample Statistics," Working Paper 20673, National Bureau of Economic Research.

Ingram, B. F. and B.-S. Lee (1991): "Simulation estimation of time-series models," *Journal of Econometrics*, 47, 197–205.

O'Rand, A. and J. Henretta (2000): *Age and Inequality: Diverse Pathways Through Later Life*, Social inequality series, Westview Press.

Song, J., D. J. Price, F. Guvenen, N. Bloom, and T. von Wachter (2015): "Firming Up Inequality," Working Paper 21199, National Bureau of Economic Research.

Figure A.1: Shock-exposure and shock-price elasticities

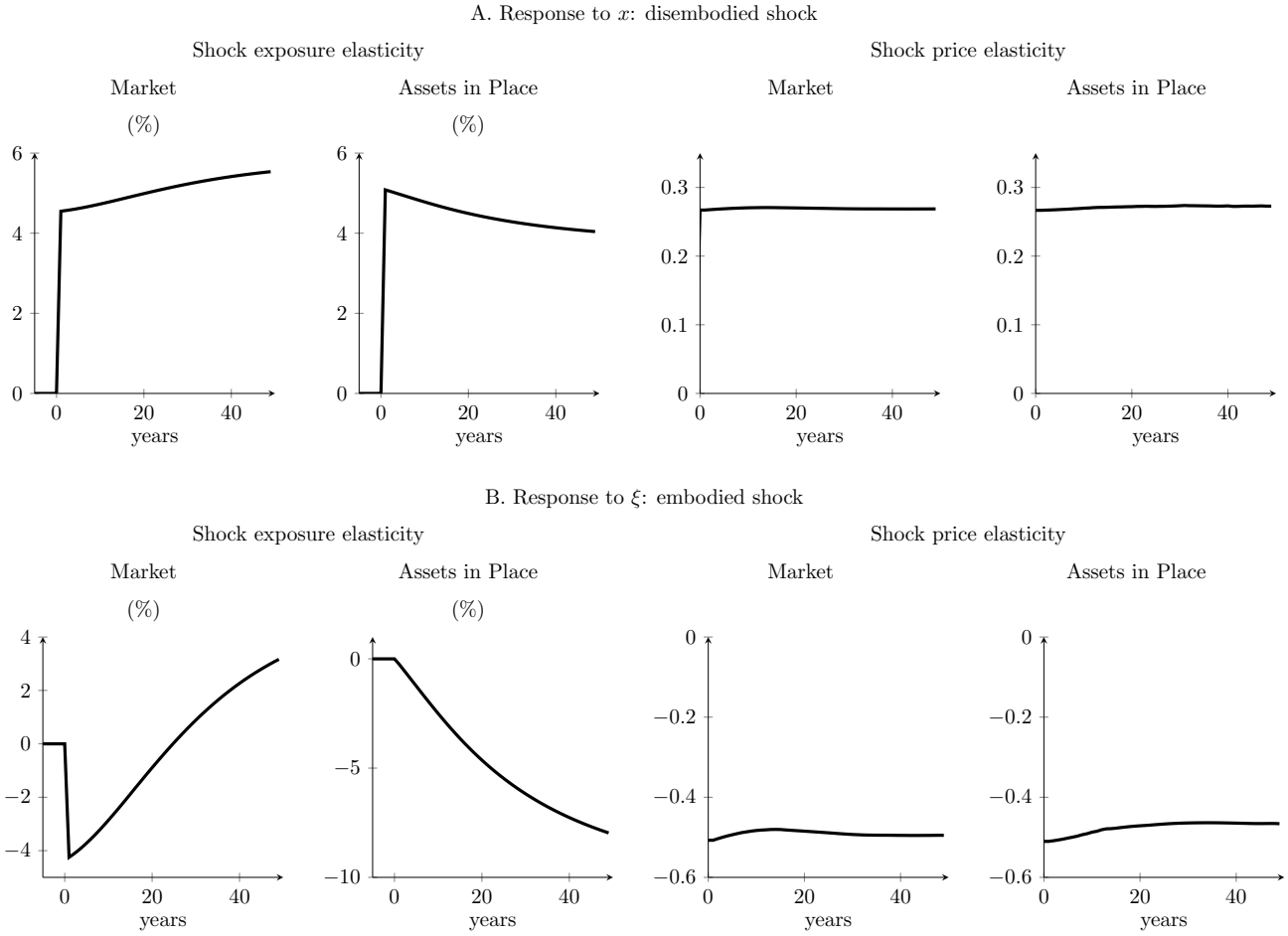

Figure plots shock-exposure and shock-price elasticities of the aggregate dividend process D, and the dividends from asset in place D^{ap} to the two technology shocks in the model. We construct the shock exposures taking into account the nonlinear nature of equilibrium dynamics: we introduce an additional shock of magnitude $\sigma\sqrt{dt}$ at time $0 + dt$ without altering the realizations of all future shocks. We then scale the resulting impulse responses by $1/\sqrt{dt}$. We compute these elasticities at the mean of the stationary distribution of ω.

Figure A.2: Firm risk exposures and risk premia

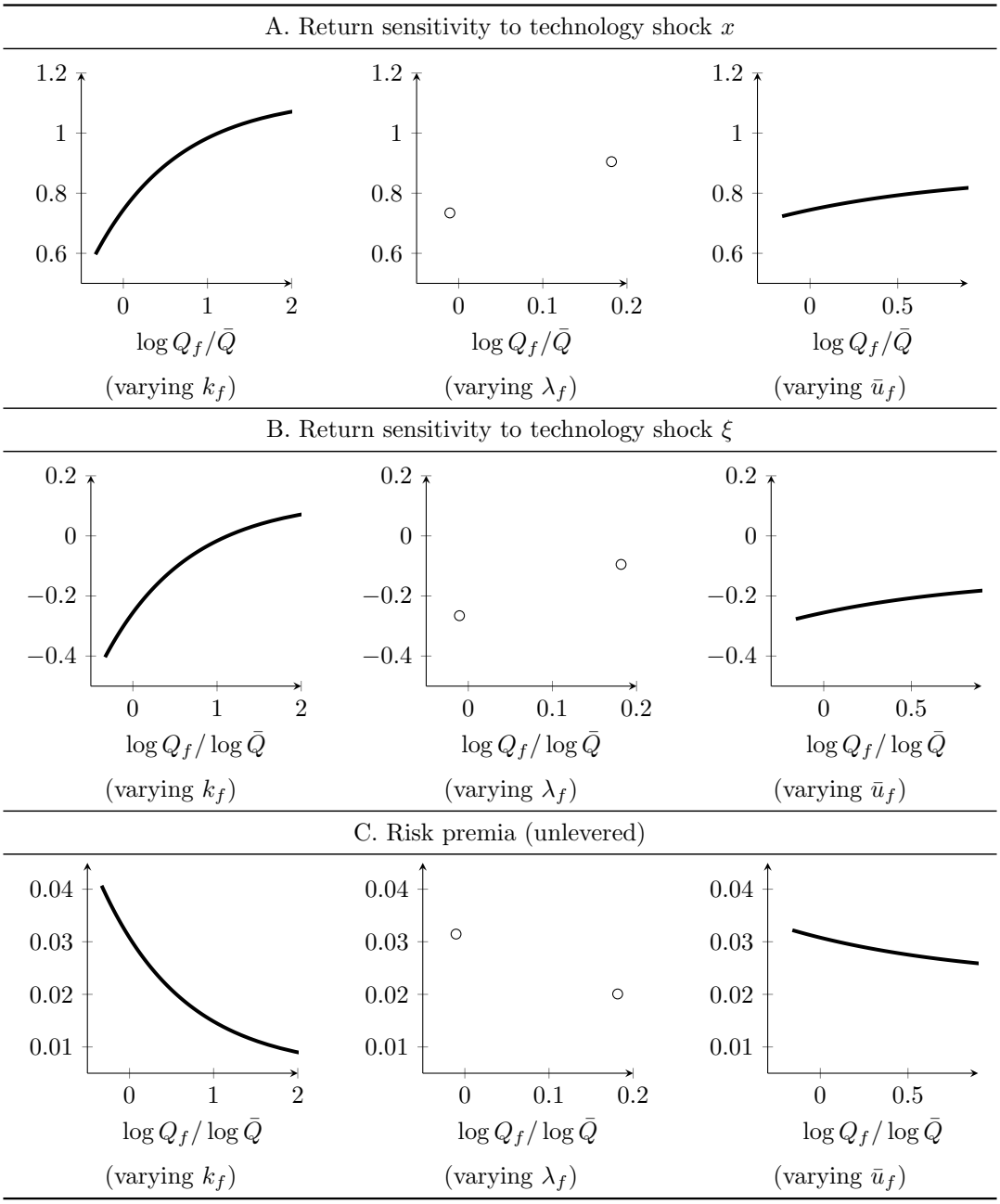

Figure illustrates how technology risk exposures (Panels A and B) and risk premia (Panel C) vary with the firm's market-to-book ratio (Q). A firm's market-to-book ratio is a function of the firm's relative size k_f, likelihood of future growth λ_f, and its current productivity $\bar{u}_f$. In each of the three columns, we examine how variation in Q due to each of these three state variables translates into variation in risk premia – while holding the other two at their average values, i.e. $\lambda_f = \lambda$, $k_f = 1$ and $\bar{u}_f = 1$. The range in the x-axis corresponds to the 0.5% and 99.5% of the range of each these three variables in simulated data. The value of the state variable ω is set to its unconditional mean, $\omega = \mathrm{E}[\omega_t]$.

Table A.1: Inequality measures: overall, vs within-cohort

Consumption Inequality (CEX)	no age effects				cubic age effects			
	all HH		stockholders		all HH		stockholders	
	overall	within cohort	overall	within cohort	overall	within cohort	overall	within cohort
99-90 ratio	1.82	1.82	1.77	1.74	1.81	1.82	1.77	1.75
99-95	1.50	1.50	1.49	1.46	1.50	1.50	1.48	1.46
95-90	1.21	1.21	1.19	1.19	1.21	1.21	1.19	1.20
90-10	4.17	4.12	3.16	3.14	4.20	4.11	3.17	3.13
90-50	1.96	1.96	1.79	1.78	1.97	1.96	1.79	1.78
50-10	2.12	2.11	1.76	1.76	2.13	2.10	1.77	1.75
Wealth Inequality (SCF)	no age effects				cubic age effects			
	all HH		stockholders		all HH		stockholders	
	overall	within cohort	overall	within cohort	overall	within cohort	overall	within cohort
99-90 ratio	7.55	6.59	6.49	5.98	6.52	6.51	5.83	5.81
99-95	4.03	3.66	3.48	3.33	3.61	3.58	3.20	3.21
95-90	1.87	1.80	1.87	1.80	1.81	1.82	1.82	1.81
90-10	154.70	94.92	50.91	29.35	94.22	91.21	29.16	28.52
90-50	7.14	6.47	5.96	5.16	6.47	6.23	5.17	5.13
50-10	21.66	14.67	8.54	5.69	14.57	14.65	5.64	5.56
Income Inequality (SCF)	no age effects				cubic age effects			
	all HH		stockholders		all HH		stockholders	
	overall	within cohort	overall	within cohort	overall	within cohort	overall	within cohort
99-90 ratio	3.86	3.82	4.42	4.29	3.71	3.77	4.31	4.27
99-95	2.71	2.66	2.96	2.89	2.61	2.65	2.87	2.88
95-90	1.42	1.44	1.49	1.49	1.42	1.42	1.50	1.48
90-10	11.36	9.68	6.76	6.30	9.84	9.07	6.28	6.03
90-50	2.96	2.79	2.62	2.56	2.76	2.70	2.52	2.50
50-10	3.84	3.47	2.58	2.46	3.57	3.35	2.49	2.41

Table reports inequality measures for consumption (using the CEX) and income or wealth (using the SCF). We first remove observation year effects from consumption, income and wealth. We then report the resulting inequality moments before and after removing cohort fixed effects. We also do so separately for the subsample of households that own stocks. Here, we define cohort effects as the birth year of the leading member of the household. We deal with the age-cohort-period identification problem in two ways. The first set of columns reports results without any age effects, so assigns the maximum amount of variation to a cohort effect. However, this may be problematic for wealth inequality, since wealth accumulation mechanically grows with age. Hence, the second column reports results after removing a cubic polynomial in age similar to Garleanu et al. (2012). Even then, the linear age effect is not identified, so we set it to zero in order to maximize the explanatory power of cohort effects.

Table A.2: Parameter boundaries for the RBF optimizer

Parameter	Symbol	Estimate	Lower Bound	Upper Bound
Preferences				
Risk aversion	γ	56.734	5	165
Elasticity of intertemporal substitution	θ	2.341	0.1	3
Effective discount rate	ρ	0.044	0.025	0.07
Preference weight on relative consumption	h	0.836	0	1
Technology				
Disembodied technology growth, mean	μ_x	0.016	0	0.05
Disembodied technology growth, volatility	σ_x	0.082	0.02	0.2
Embodied technology growth, mean	μ_ξ	0.004	0	0.05
Embodied technology growth, volatility	σ_ξ	0.110	0.02	0.2
Project-specific productivity, long-run volatility	v_u	1.981	0.1	2.5
Project-specific productivity, mean reversion	κ_u	0.210	0.1	0.5
Production and Investment				
Cobb-Douglas capital share	ϕ	0.427		
Decreasing returns to investment	α	0.446	0.1	0.9
Depreciation rate	δ	0.029	0.01	0.1
Transition rate to low-growth state	μ_L	0.364	0.005	0.75
Transition rate to high-growth state	μ_H	0.021	0.005	0.75
Project mean arrival rate, mean	λ	0.812	0.1	3
Project mean arrival rate, rel. difference high-low growth states	λ_D	15.674	0.1	100
Incomplete Markets				
Fraction of project NPV that goes to inventors	η	0.767	0	1
Fraction of households that is a shareholder	ψ	0.148	0.04	1

Table reports the parameter bounds that we used in our implementation of the RBF search algorithm.

Table A.3: Robustness across restricted models: Goodness of Fit

	DATA	BASE	FullPart	Restrict η			Restrict h			No ξ	Restrict γ
			$\psi = 1$	$\eta = 0$	$\eta \leq 0.3$	$\eta \leq 0.6$	$h = 0$	$h \leq 0.3$	$h \leq 0.6$		$\gamma \leq 10$
Aggregate quantities											
Consumption growth, mean	0.015	0.014	0.013	0.012	0.013	0.014	0.015	0.016	0.014	0.010	0.013
Consumption growth, volatility (short-run)	0.036	0.039	0.039	0.041	0.039	0.039	0.037	0.033	0.037	0.038	0.039
Consumption growth, volatility (long-run)	0.041	0.053	0.053	0.055	0.052	0.054	0.052	0.047	0.051	0.048	0.054
Shareholder consumption share, mean	0.429	0.464	-	0.320	0.406	0.449	0.408	0.409	0.397	0.443	0.399
Shareholder consumption growth, volatility	0.037	0.039	-	0.044	0.039	0.039	0.039	0.036	0.039	0.036	0.042
Investment-to-output ratio, mean	0.089	0.083	0.070	0.094	0.075	0.080	0.082	0.081	0.084	0.100	0.090
Investment-to-output ratio (log), volatility	0.305	0.288	0.282	0.325	0.305	0.291	0.312	0.315	0.304	0.025	0.312
Investment growth, volatility	0.130	0.105	0.101	0.119	0.108	0.107	0.112	0.110	0.109	0.048	0.108
Investment and consumption growth, correlation	0.472	0.373	0.378	0.401	0.390	0.386	0.275	0.182	0.314	0.998	0.315
Aggregate Innovation, volatility	0.370	0.369	0.371	0.397	0.362	0.362	0.397	0.383	0.380	0.123	0.430
Capital share, mean	0.356	0.354	0.323	0.373	0.394	0.363	0.315	0.328	0.342	0.353	0.303
Asset Prices											
Market portfolio, excess returns, mean	0.063	0.067	0.068	0.053	0.066	0.071	0.081	0.089	0.078	0.053	0.039
Market portfolio, excess returns, volatility	0.185	0.131	0.138	0.132	0.125	0.129	0.139	0.119	0.128	0.116	0.161
Risk-free rate, mean	0.020	0.020	0.022	0.020	0.022	0.022	0.024	0.022	0.022	0.026	0.023
Risk-free rate, volatility	0.007	0.007	0.007	0.008	0.007	0.007	0.006	0.005	0.006	0.002	0.007
Value factor, mean	0.065	0.063	0.051	0.034	0.056	0.059	0.014	0.041	0.052	-0.010	0.050
Value factor, volatility*	0.243	0.152	0.184	0.122	0.138	0.143	0.274	0.263	0.196	0.088	0.223
Value factor, CAPM alpha*	0.050	0.046	0.031	0.034	0.044	0.045	-0.004	0.016	0.026	-0.003	0.030
Cross-sectional moments											
Investment rate, IQR	0.175	0.163	0.174	0.155	0.159	0.163	0.174	0.172	0.164	0.101	0.188
Investment rate, persistence	0.223	0.228	0.204	0.230	0.213	0.226	0.171	0.154	0.200	0.179	0.209
Tobin Q, IQR	1.139	0.882	0.816	1.046	1.125	0.978	0.562	0.874	0.874	0.663	0.926
Tobin Q, persistence	0.889	0.948	0.940	0.951	0.951	0.952	0.899	0.933	0.942	0.947	0.946
Firm innovation, 90-50 range	0.581	0.542	0.602	0.633	0.575	0.530	0.667	0.701	0.621	0.683	0.640
Firm innovation, persistence	0.551	0.567	0.552	0.560	0.585	0.595	0.502	0.550	0.601	0.489	0.633
Profitability, IQR	0.902	0.936	0.948	0.917	0.925	0.927	0.923	0.944	0.911	0.675	0.966
Profitability, persistence	0.818	0.815	0.772	0.844	0.825	0.857	0.765	0.849	0.779	0.861	0.792
		0.014	0.020	0.024	0.015	0.015	0.061	0.050	0.022	0.240	0.028

Starred moments are not part of the estimation targets. They are included here for comparison.

Table A.4: Robustness across restricted models: Parameters

Parameter	symbol	BASE	$\psi = 1$	$\eta = 0$	$\eta \leq 0.3$	$\eta \leq 0.6$	$h = 0$	$h \leq 0.3$	$h \leq 0.6$	No ξ	Restrict γ
Preference											
Risk aversion	γ	56.73	104.57	92.80	83.35	72.49	15.74	30.85	34.34	73.37	10.00
Elasticity of intertemporal substitution	θ	2.34	2.30	2.15	1.96	1.87	0.82	1.50	1.81	1.73	2.75
Effective discount rate	ρ	0.04	0.04	0.04	0.05	0.05	0.06	0.06	0.05	0.05	0.04
Preference weight on relative consumption	h	0.84	0.93	0.92	0.89	0.85	0.00	0.30	0.60	0.85	0.99
Technology Shocks											
Disembodied technology growth, mean	μ_x	0.02	0.02	0.01	0.02	0.02	0.01	0.02	0.01	0.01	0.02
Disembodied technology growth, volatility	σ_x	0.08	0.08	0.08	0.08	0.08	0.08	0.07	0.08	0.08	0.08
Embodied technology growth, mean	μ_ξ	0.00	0.00	0.00	0.00	0.00	0.01	0.00	0.01	-	0.00
Embodied technology growth, volatility	σ_ξ	0.11	0.12	0.11	0.11	0.11	0.12	0.12	0.11	-	0.13
Project-specific productivity, mean reversion	κ_u	0.21	0.28	0.17	0.20	0.15	0.29	0.16	0.27	0.11	0.25
Project-specific productivity, volatility	σ_u	0.53	0.61	0.47	0.51	0.44	0.61	0.46	0.58	0.32	0.58
Production and Investment											
Decreasing returns to investment	α	0.45	0.36	0.58	0.46	0.45	0.39	0.40	0.45	0.35	0.41
Depreciation rate	δ	0.03	0.03	0.03	0.03	0.03	0.03	0.03	0.03	0.08	0.03
Cobb Douglas Capital Share	ϕ	0.43	0.42	0.37	0.41	0.42	0.43	0.43	0.42	0.40	0.43
Transition rate to low-growth state	μ_L	0.36	0.26	0.19	0.19	0.35	0.23	0.13	0.23	0.41	0.12
Transition rate to high-growth state	μ_H	0.02	0.02	0.01	0.01	0.02	0.02	0.01	0.02	0.01	0.01
Project mean arrival rate, mean	λ	0.81	0.70	0.60	0.68	0.91	0.86	1.00	0.97	3.61	1.05
—, diff. high-low growth states	λ_D	15.67	13.98	15.32	16.55	13.41	11.44	12.32	13.14	29.75	12.06
Incomplete Markets											
Fraction of population that is a shareholder	ψ	0.14	-	0.05	0.06	0.13	0.05	0.05	0.05	0.16	0.05
Fraction of project NPV that goes to inventors	η	0.77	0.81	0.00	0.30	0.60	0.86	0.84	0.75	0.27	0.95

Figure A.3: Sensitivity of parameters to moments (GS)

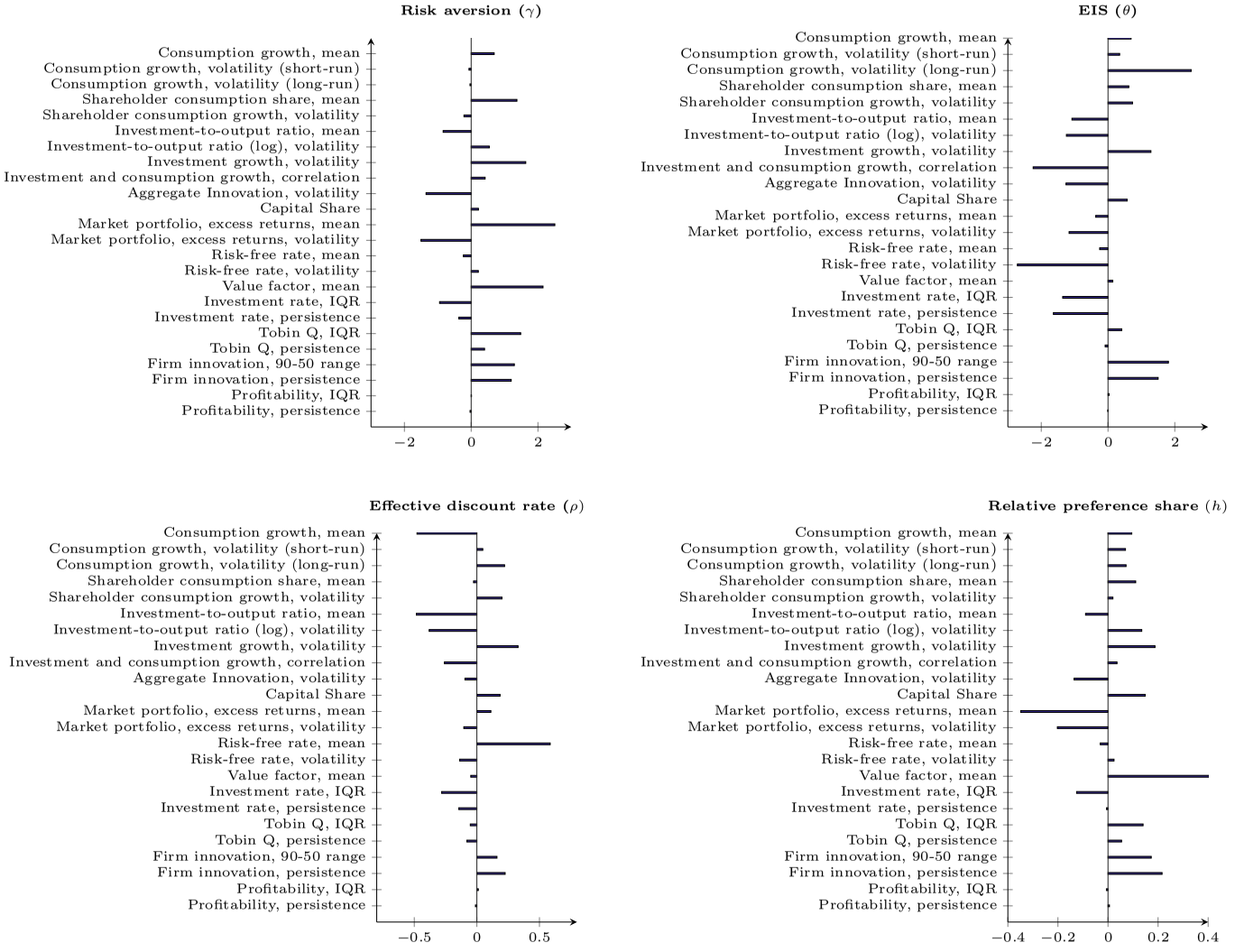

We report the Gentzkow and Shapiro (2014) sensitivity measure of the estimated parameters to moments. We report the measure in elasticity form, $\lambda_{i,j}\frac{X^j}{\theta^i}$, where $\lambda_{i,j}$ is the element of the sensitivity matrix Λ that corresponds to parameter i and moment j.

Figure A.4: Sensitivity of parameters to moments (GS)

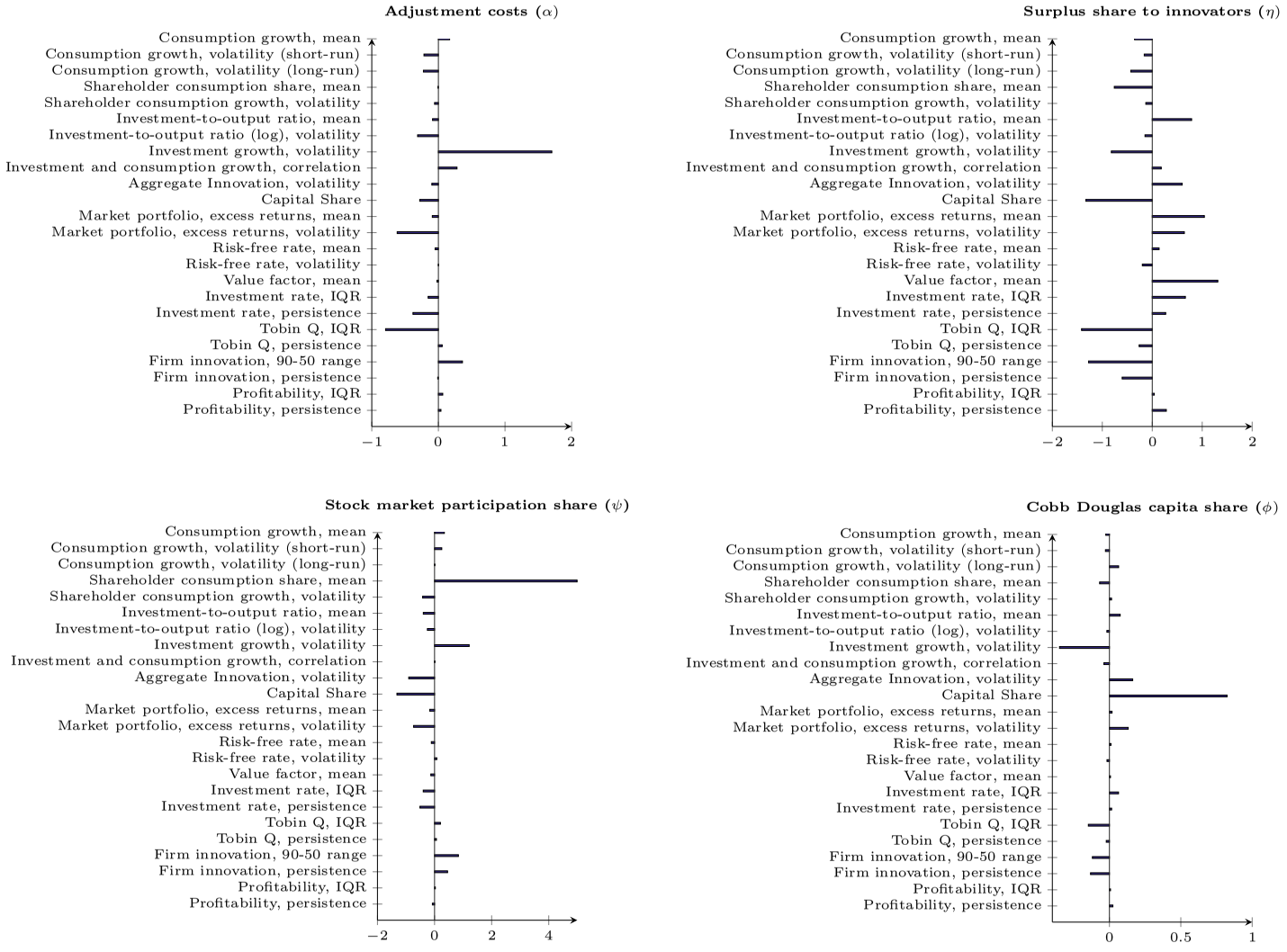

We report the Gentzkow and Shapiro (2014) sensitivity measure of the estimated parameters to moments. We report the measure in elasticity form, $\lambda_{i,j}\frac{X^j}{\theta^i}$, where $\lambda_{i,j}$ is the element of the sensitivity matrix Λ that corresponds to parameter i and moment j.

Figure A.5: Sensitivity of parameters to moments (GS)

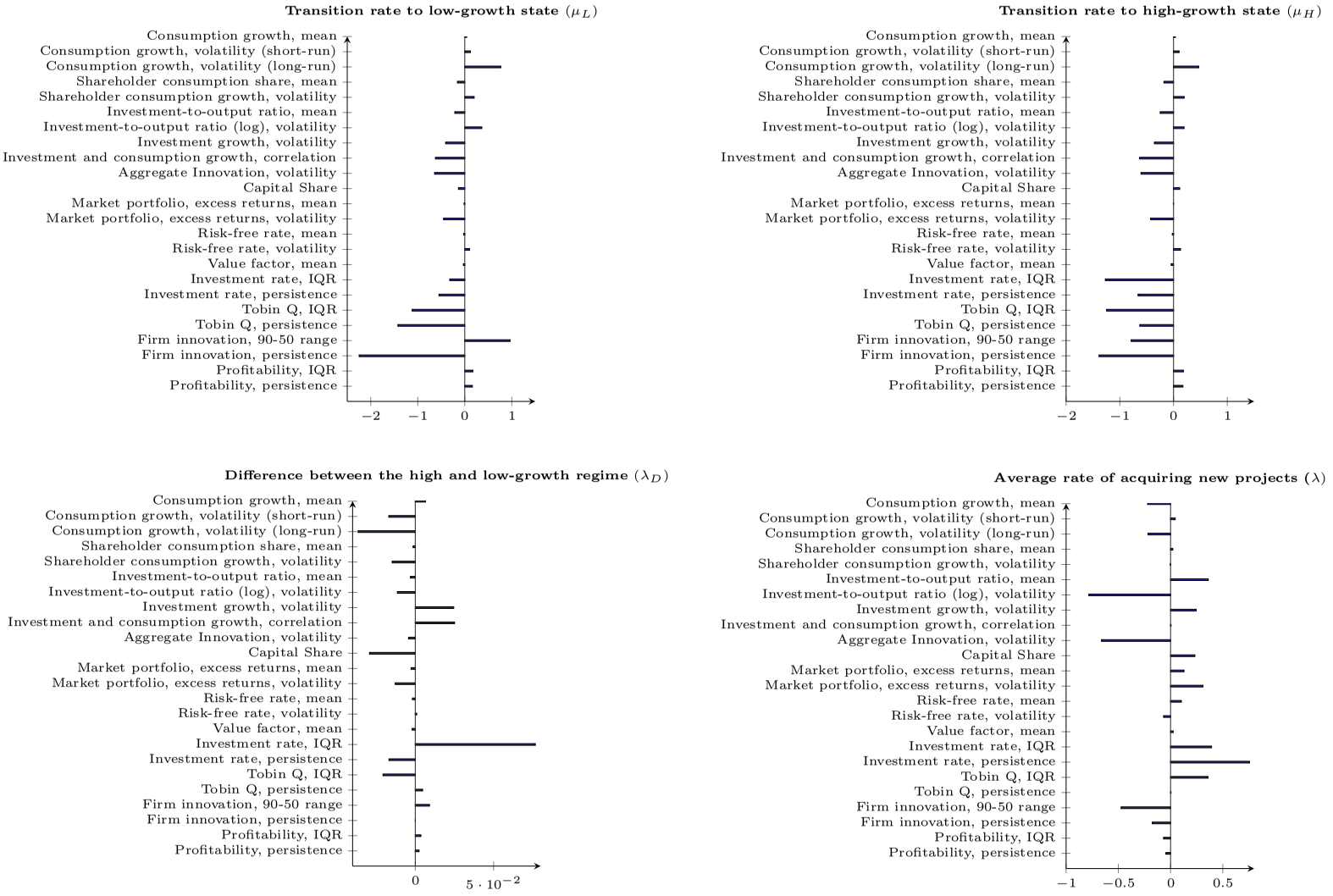

We report the Gentzkow and Shapiro (2014) sensitivity measure of the estimated parameters to moments. We report the measure in elasticity form, $\lambda_{i,j} \frac{X^j}{\theta^i}$, where $\lambda_{i,j}$ is the element of the sensitivity matrix Λ that corresponds to parameter i and moment j.

Figure A.6: Sensitivity of parameters to moments (GS)

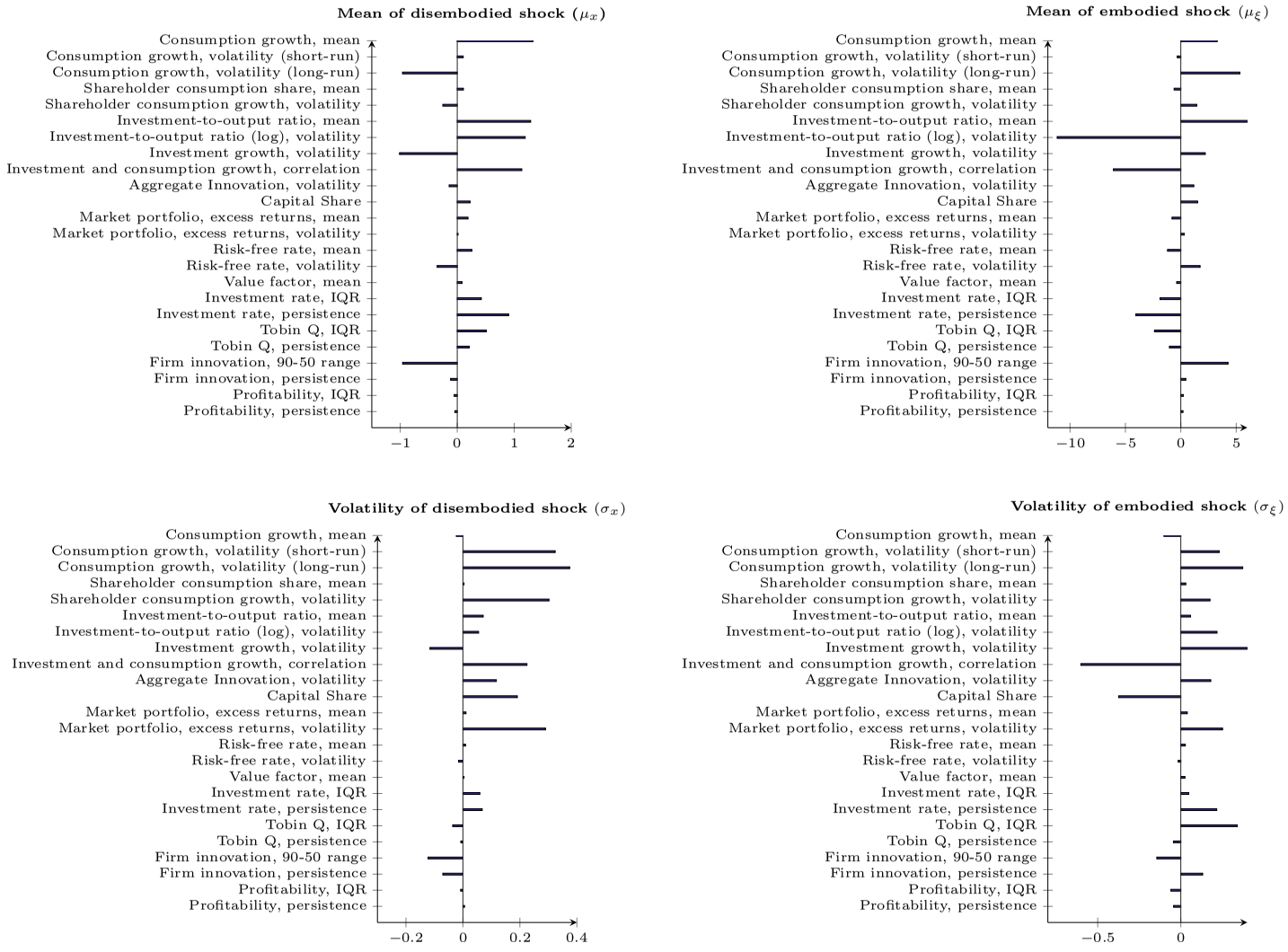

We report the Gentzkow and Shapiro (2014) sensitivity measure of the estimated parameters to moments. We report the measure in elasticity form, $\lambda_{i,j}\frac{X^j}{\theta^i}$, where $\lambda_{i,j}$ is the element of the sensitivity matrix Λ that corresponds to parameter i and moment j.

Figure A.7: Sensitivity of parameters to moments (GS)

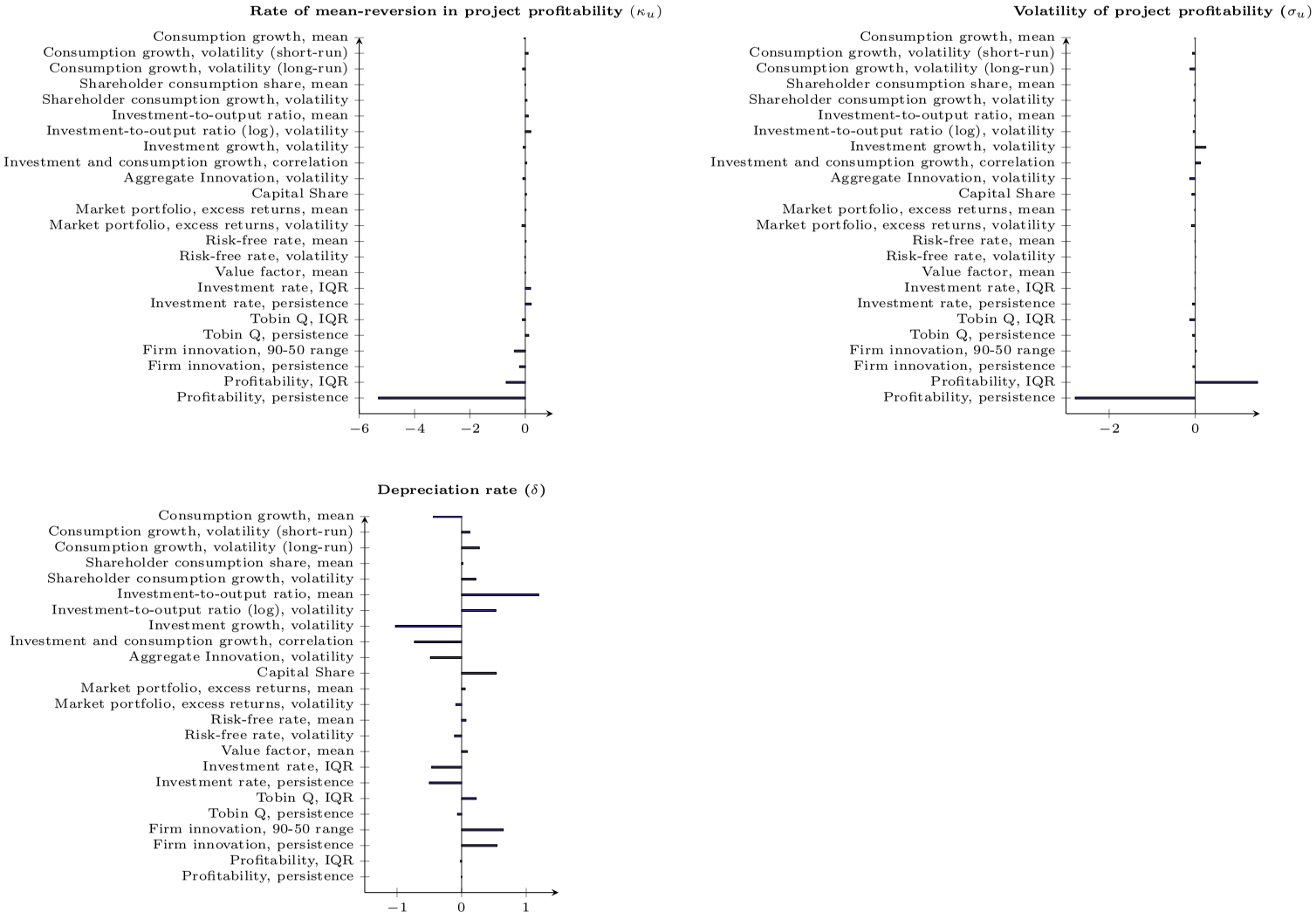

We report the Gentzkow and Shapiro (2014) sensitivity measure of the estimated parameters to moments. We report the measure in elasticity form, $\lambda_{i,j}\frac{X^j}{\theta^i}$, where $\lambda_{i,j}$ is the element of the sensitivity matrix Λ that corresponds to parameter i and moment j.